© 2014. Published by The Company of Biologists Ltd | Development (2014) 141, 410-421 doi:10.1242/dev.095984

RESEARCH ARTICLE

PTK7 modulates Wnt signaling activity via LRP6

Naama Bin-Nun, Hava Lichtig, Anastasia Malyarova, Michal Levy, Sara Elias and Dale Frank*

ABSTRACT

Protein tyrosine kinase 7 (PTK7) is a transmembrane protein expressed in the developing *Xenopus* neural plate. PTK7 regulates vertebrate planar cell polarity (PCP), controlling mesodermal and neural convergent-extension (CE) cell movements, neural crest migration and neural tube closure in vertebrate embryos. Besides CE phenotypes, we now show that PTK7 protein knockdown also inhibits Wnt/β-catenin activity. Canonical Wnt signaling caudalizes the neural plate via direct transcriptional activation of the *meis3* TALE-class homeobox gene, which subsequently induces neural CE. PTK7 controls *meis3* gene expression to specify posterior tissue and downstream PCP activity. Furthermore, PTK7 morphants phenocopy embryos depleted for Wnt3a, LRP6 and Meis3 proteins. PTK7 protein depletion inhibits embryonic Wnt/β-catenin signaling by strongly reducing LRP6 protein levels. LRP6 protein positively modulates Wnt/β-catenin, but negatively modulates Wnt/PCP activities. The maintenance of high LRP6 protein levels by PTK7 triggers PCP inhibition. PTK7 and LRP6 proteins physically interact, suggesting that PTK7 stabilization of LRP6 protein reciprocally regulates both canonical and noncanonical Wnt activities in the embryo. We suggest a novel role for PTK7 protein as a modulator of LRP6 that negatively regulates Wnt/PCP activity.

KEY WORDS: Protein tyrosine kinase 7 (PTK7), Wnt/β-catenin, Planar cell polarity, LRP6 protein, *Xenopus*, Neural patterning

INTRODUCTION

Wnt signaling regulates many embryonic and adult physiological processes. The most characterized Wnt-network pathway is the Wnt/β-catenin/canonical pathway. Secreted Wnt ligands bind receptor complexes composed of the Frizzled (Fz) seven transmembrane receptor and the low-density lipoprotein receptor-related protein 6 (LRP6). Following Wnt-ligand binding, LRP6 undergoes phosphorylation, recruiting Axin protein to the membrane in a disheveled (Dvl) protein-dependent manner. Dvl and Axin bind GSK3β, preventing β-catenin phosphorylation and degradation. β-catenin translocates to the nucleus, where it binds TCF/LEF proteins to directly activate target gene transcription (MacDonald et al., 2009).

LRP6 function is dependent on dimerization with Fz and the intracellular phosphorylation of its multiple PPPSPXS domains and S/T motifs (Bilic et al., 2007; MacDonald et al., 2008). Upon Wnt/Fz/LRP6 complex formation, Axin and GSK3β are recruited to the membrane, where GSK3β and CK1γ phosphorylate LRP6 (Davidson et al., 2005; Bilic et al., 2007; Zeng et al., 2008). Phosphorylation sites serve as additional docking sites for Axin and GSK3β, freeing more β-catenin. LRP6 phosphorylation triggers auto-oligomerization, creating 'LRP6-signalosomes' that recruit more LRP6 to amplify the Wnt signal (Niehrs and Shen, 2010).

In *Xenopus*, Wnt/β-catenin acts in two distinct temporal patterning pathways. Maternal activation induces the Spemann organizer in the dorsal mesoderm (Niehrs, 2004). Later zygotic Wnt/β-catenin signaling caudalizes anterior neural cells to posterior fates (Elkouby and Frank, 2010). In the posterior neural plate, both zygotic canonical and noncanonical Wnt activities regulate cell fate specification and morphogenesis. Mesodermal Wnt3a protein induces *meis3* TALE-class homeobox gene expression in the posterior neural plate, which specifies hindbrain, primary neuron and neural crest fates (Salzberg et al., 1999; Gutkovich et al., 2010). Meis3 protein subsequently activates noncanonical Wnt planar cell polarity (PCP) activity, inducing posterior neural convergent-extension (CE) cell movements (Aamar and Frank, 2004). Thus, canonical Wnt signaling acts upstream of Wnt-PCP via *meis3* gene expression (Elkouby et al., 2010).

LRP6 protein bridges canonical- and PCP-Wnt activities to modulate CE movements in the *Xenopus* neural plate; either ectopic or reduced LRP6 levels inhibit neural CE (Tahinci et al., 2007). Tightly balanced PCP activity optimizes cell polarity. CE is perturbed when PCP is inhibited, but PCP overstimulation by pathway activators also disrupts cell-polarization activity, preventing cell intercalations (Wallingford et al., 2000; Djiane et al., 2000). LRP6 protein modulates CE via Wnt-PCP activity. In excess, LRP6 inhibits PCP, yet when depleted, LRP6 overstimulates PCP; thus CE movements are inhibited (Tahinci et al., 2007; Bryja et al., 2009). Additionally, LRP6 depletion lowers canonical Wnt signaling in the neural plate, disrupting posterior neural cell fate specification, reducing CE. Two possible nonmutually exclusive mechanisms explain neural CE inhibition by LRP6. Posterior neural cells that typically undergo CE are lost, and/or a parallel inhibitory spike of Wnt-PCP activity is released by LRP6 loss of function. This complex dual-regulation of Wnt/β-catenin and PCP activities by LRP6 must be analyzed to elucidate LRP6 function in loss- or gain-of-function phenotypes.

Protein tyrosine kinase 7 (PTK7), a transmembrane protein lacking an active kinase domain, is structurally conserved among vertebrates and invertebrates (Miller and Steele, 2000). In PTK7 mutant mice, gastrulation cell movements are disrupted, neural tube closure is perturbed and stereociliary bundle orientation in the inner ear is disturbed (Lu et al., 2004; Yen et al., 2009; Paudyal et al., 2010). The *Xenopus ptk7* homolog is expressed in the neural plate and its knockdown disrupts neural tube closure and CE (Lu et al., 2004). These phenotypes resemble known Wnt-PCP mutations, suggesting that PTK7 regulates PCP activity in vertebrates.

We show that PTK7 protein knockdown not only disrupts neural CE, but strongly inhibits posterior neural cell fate specification. PTK7-morphant embryos have a zygotic canonical Wnt loss-of-function phenotype. PTK7 protein depletion inhibits Wnt ligand or LRP6 induction of β-catenin direct-target gene expression in

Department of Biochemistry, The Rappaport Family Institute for Research in the Medical Sciences, Faculty of Medicine, Technion – Israel Institute of Technology, Haifa 31096, Israel.

*Author for correspondence (dale@tx.technion.ac.il)

Received 27 February 2013; Accepted 28 October 2013

Development (2014) doi:10.1242/dev.095984

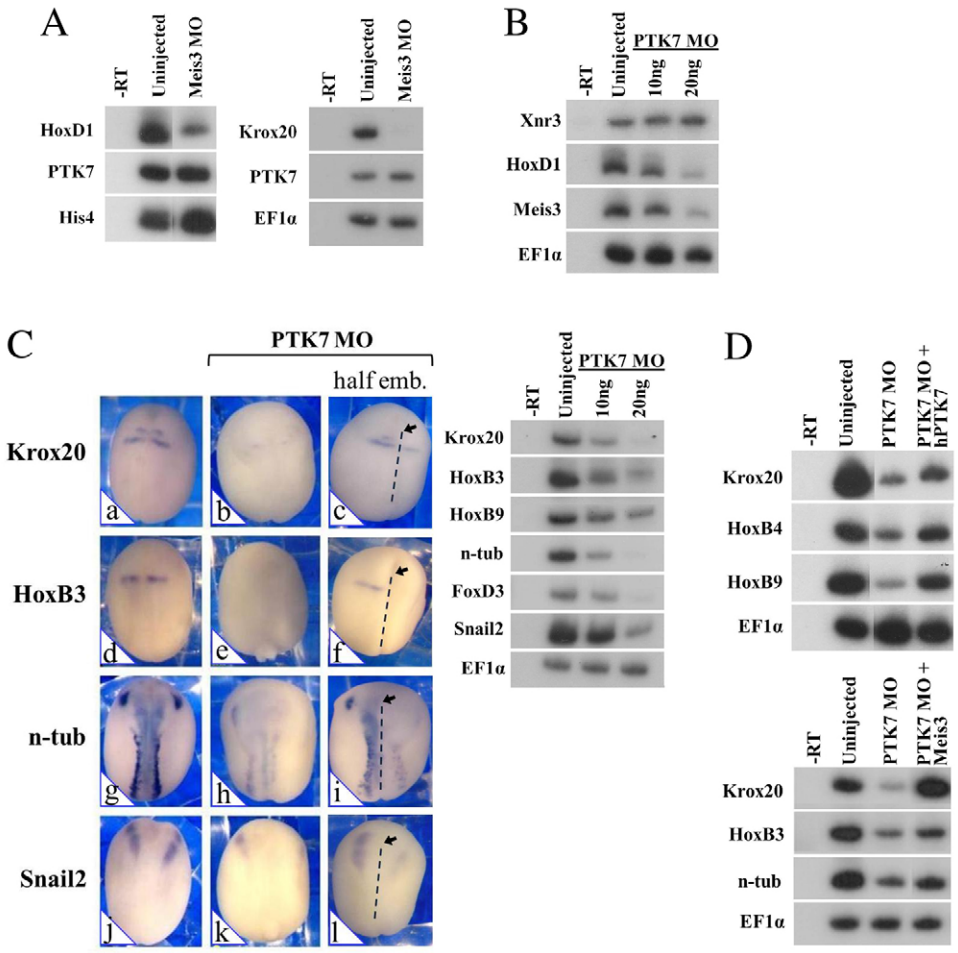

Fig. 1. PTK7 protein is required for posterior neural cell fate specification. (A) Left panel: sqRT-PCR to pools of ten early-neurula (st.12) embryos injected with 15 ng *Meis3*-MO at the one-cell stage. *HoxD1* expression inhibition is as a positive control for *Meis3*-MO activity. *His4* controls for RNA levels. A control PCR omitting reverse transcriptase (–RT) was performed on RNA isolated from control embryos in all experiments shown. Right panel: sqRT-PCR to pools of five neurula (st.19) embryos injected with 22 ng *Meis3*-MO at the one-cell stage. *Krox20* expression inhibition is a positive control for *Meis3*-MO activity. *EF1α* controls for RNA levels. (B) sqRT-PCR to pools of six early-neurula (st.12.5) embryos injected with 10-20 ng *PTK7*-MO at the one-cell stage. (C) Left panel: embryos were injected into one blastomere at either the one- or two-cell stage with *PTK7*-MO (12 or 6 ng, respectively). Four posterior cell-type markers were analyzed by *in situ* hybridization. Neurula embryos (st.17), viewed dorsally, anterior is on top. Arrows and dashed line mark the dorsal midline; two-cell-stage embryos injected on right side. *Krox20* expression (a) is normal in 100% of the control embryos (*n*=21) and perturbed (b,c) in 78% of the PTK7-morphant embryos (*n*=46). *HoxB3* expression (d) is normal in all of the controls (*n*=23) and perturbed (e,f) in 98% of the PTK7 morphants (*n*=46). *N-tub* expression is normal (g) in all controls (*n*=23) and perturbed (h,i) in 95% of the morphants (*n*=44). *Snail2* expression is normal (j) in all controls (*n*=20) and perturbed (k,l) in 87% of the morphants (*n*=46). Right panel: sqRT-PCR to pools of six neurula (st.19) embryos injected at the one-cell stage with *PTK7*-MO (10 or 20 ng). (D) Upper panel: sqRT-PCR to pools of eight neurula (st.17) embryos injected at the one-cell stage with *PTK7*-MO (12 ng) and RNA encoding the human PTK7 protein (100 pg). Lower panel: sqRT-PCR to pools of seven neurula (st.16) embryos injected at the one-cell stage with *PTK7*-MO (10 ng) and RNA encoding the Meis3 protein (1.1 ng).

embryos, explants and cultured cells. PTK7 protein depletion strongly reduces LRP6 protein levels in embryos and explants. LRP6 and PTK7 are both transmembrane proteins that physically interact in both *Xenopus* and cultured cells. PTK7 and LRP6 proteins appear to interact via their transmembrane domains, probably stabilizing LRP6 protein levels. In *Xenopus*, PTK7 protein depletion phenocopies the LRP6 knockdown phenotype. Although most previous studies suggest an exclusive role for PTK7 as a positive modulator of PCP activity driving cell morphogenesis, we alternatively suggest that PTK7 protein acts to regulate LRP6 protein levels. LRP6 protein acts at a crucial crossroads to fine-tune both canonical- and PCP-Wnt activity levels, coordinating cell fate specification and morphogenesis during early development.

RESULTS

Role of PTK7 protein in early neural patterning

As PTK7 and Meis3 proteins both regulate neural plate CE movements, we examined Meis3/PTK7 epistasis. *ptk7* gene expression was unchanged in Meis3-morphant embryos at early-neurula stages (Fig. 1A). However, in PTK7 morphants, *meis3* gene expression was severely repressed at similar stages (Fig. 1B). Canonical Wnt/β-catenin-activity directly induces *meis3* expression to control posterior neural cell fates (Elkouby et al., 2010), so we determined if posterior neural cell fates were also lost in PTK7 morphants. As assayed by marker expression, both early and late expressed hindbrain, neural crest and primary neuron fates were lost in PTK7 morphants (Fig. 1B,C). At early-neurula stages, similar to *meis3*, *hoxd1* gene expression is also highly reduced

Development (2014) doi:10.1242/dev.095984

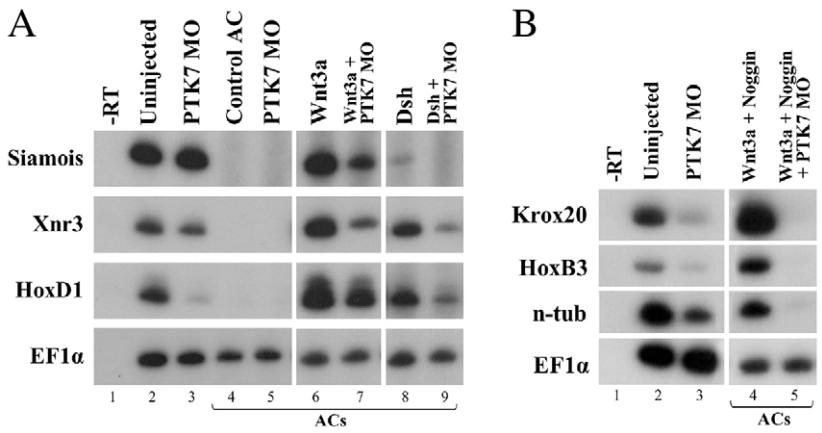

Fig. 2. PTK7 protein depletion inhibits canonical Wnt-pathway activation. (A) Embryos were injected at the one-cell stage with *PTK7*-MO (12 ng) and RNAs encoding Wnt3a (4 pg) or Dvl (1 ng) proteins. AC explants were removed from control and injected embryos at the blastula stage and grown to gastrula st.10.5. Total RNA was isolated from five control and *PTK7*-MO-injected embryos (lanes 2,3) and 18 ACs from each group (lanes 4-9). Wnt direct-target genes examined by sqRT-PCR: *siamois*, *xnr3* and *hoxd1*. In embryos, *hoxd1* expression inhibition is a positive control for *PTK7*-MO activity. (B) RNAs encoding Wnt3a (7 pg) and Noggin (7 pg) proteins were injected at the one-cell stage with *PTK7*-MO (13 ng). ACs removed at the blastula stage were grown to neurula st.16, when total RNA was isolated from five control and injected embryos (lanes 2,3) and 18 explants from each AC group (lanes 4,5). In embryos, reduction in posterior neural marker expression is a positive control for *PTK7*-MO activity.

(Fig. 1B); *hoxD1* is a direct-target gene of both Meis3 and β-catenin proteins (Dibner et al., 2004; Janssens et al., 2010). At later neurula stages, hindbrain (*krox20*, *hoxb3*), neural crest (*snail2*), and primary neuron (*n-tub*) marker expression is strongly inhibited (Fig. 1C; Fig. 2B; Fig. 4D), suggesting a phenotype more similar to a loss of canonical Wnt/β-catenin signaling than noncanonical Wnt-PCP signaling. These results phenocopy other zygotic canonical Wnt phenotypes, such as Meis3 or Wnt3a protein knockdown, or ectopic Dkk1 protein expression (Elkouby et al., 2010). In PTK7-morphant embryos, we never observe reduced expression of early maternal Wnt direct-target genes (*siamois* or *xnr3*) expressed in the organizer (Fig. 1B; Fig. 2A; Fig. 3A,B). *PTK7*-morpholino oligonucleotide (*PTK7*-MO) effects are specific; the loss-of-posterior cell fate phenotype is rescued by ectopic expression of Meis3 or human PTK7 proteins (Fig. 1D). These results suggest that in addition to regulating Wnt-PCP, PTK7 knockdown compromises some signaling component of the Wnt/β-catenin pathway.

PTK7 protein depletion inhibits canonical Wnt signaling

To understand PTK7 regulation of Wnt/β-catenin activity, we utilized the *Xenopus* animal cap (AC) assay. In ACs, ectopic canonical Wnt-pathway components activate transcription of the β-catenin direct-target genes, *xnr3* and *siamois*. In the embryo, *xnr3* and *siamois* gene expression is dependent on maternal, but not zygotic Wnt ligands and receptors. In ACs, transcription of *xnr3* and *siamois* is dependent on zygotic Wnt-pathway components. In ACs, co-injection of the *PTK7*-MO sharply decreased Wnt3a-induced *xnr3* and *siamois* expression (Fig. 2A, lanes 4-7). Expression of the early neural Wnt target gene, *hoxd1* was also strongly inhibited (Fig. 2A, lanes 4-7). Also, in PTK7-depleted ACs, induction of markers by ectopic Dvl is inhibited (Fig. 2A, lanes, 8,9). In PTK7-morphant embryos, endogenous zygotic *hoxd1* gene expression is repressed, but maternally regulated *siamois* and *xnr3* gene expression is unchanged (Fig. 2A, lanes 2,3; see also Fig. 3A,B; Fig. 4D). In ACs caudalized by co-injection of Wnt3a and noggin proteins, PTK7 depletion strongly inhibited Wnt-dependent posterior neural marker expression, such as *krox20*, *hoxb3* and *n-tubulin*, thus recapitulating in ACs the embryonic PTK7-morphant phenotype (Fig. 2B, lanes 4,5).

Depletion of PTK7 protein inhibits LRP6 activity

Canonical Wnt ligands signal via the Fz/LRP6 receptor complex. As PTK7 is a transmembrane protein, we examined potential LRP6/PTK7 interactions. In PTK7-depleted AC explants, both wild-type LRP6 and constitutively activated amino-truncated LRP6ΔN/LRP6ΔE1-4 proteins could not induce expression of Wnt target genes (Fig. 3A). LRP6ΔN protein robustly activates the canonical Wnt pathway independently of Wnt and Dvl proteins (Cong et al., 2004). Indeed, whereas Wnt ligand activity is sensitive to both PTK7 depletion and Dvl protein inhibition by the Xdd1 dominant-negative Dvl protein (Fig. 3B, lanes 8-10), the constitutive-active LRP6 receptor protein is significantly more sensitive to PTK7 protein depletion than Dvl activity inhibition by co-expression of the Xdd1 protein (Fig. 3B, lanes 1-13). In general, the LRP6ΔN protein seems more sensitive to the loss of PTK7 protein than the Wnt ligand. The observation that PTK7 protein knockdown promotes such a severe inhibitory effect on LRP6ΔN activity suggests that wild-type LRP6 protein activity may be regulated by PTK7.

Unlike wild-type LRP6 protein, the LRP6ΔN/ΔE1-4 proteins are Wnt ligand independently hyper-phosphorylated *in vivo* by CK1-γ and GSK3 (Bilic et al., 2007; Zeng et al., 2008), activating the intracellular Wnt pathway. We determined whether LRP6 phosphorylation was reduced in PTK7-depleted explants using the Tp1479 antibody (Bilic et al., 2007). Surprisingly, overall LRP6ΔN protein levels were highly reduced by PTK7 protein depletion (Fig. 3C).

To complement experiments in *Xenopus*, we used shRNA-PTK7 to deplete endogenous PTK7 protein in human HEK293 cells (Fig. 3D). PTK7 protein depletion strongly inhibited LRP6 activation of the *TOP-Flash* (β-catenin/Wnt-dependent) reporter vector (Fig. 3D). LRP6 protein levels were also reduced in these experiments (not shown). In the presence of the shRNA-PTK7, co-expression of the heterologous *Xenopus* PTK7 protein rescued LRP6 induction of the reporter (Fig. 3D). These results show that in addition to *Xenopus*, PTK7 is required for LRP6-dependent induction of canonical Wnt activity in human cells.

Development (2014) doi:10.1242/dev.095984

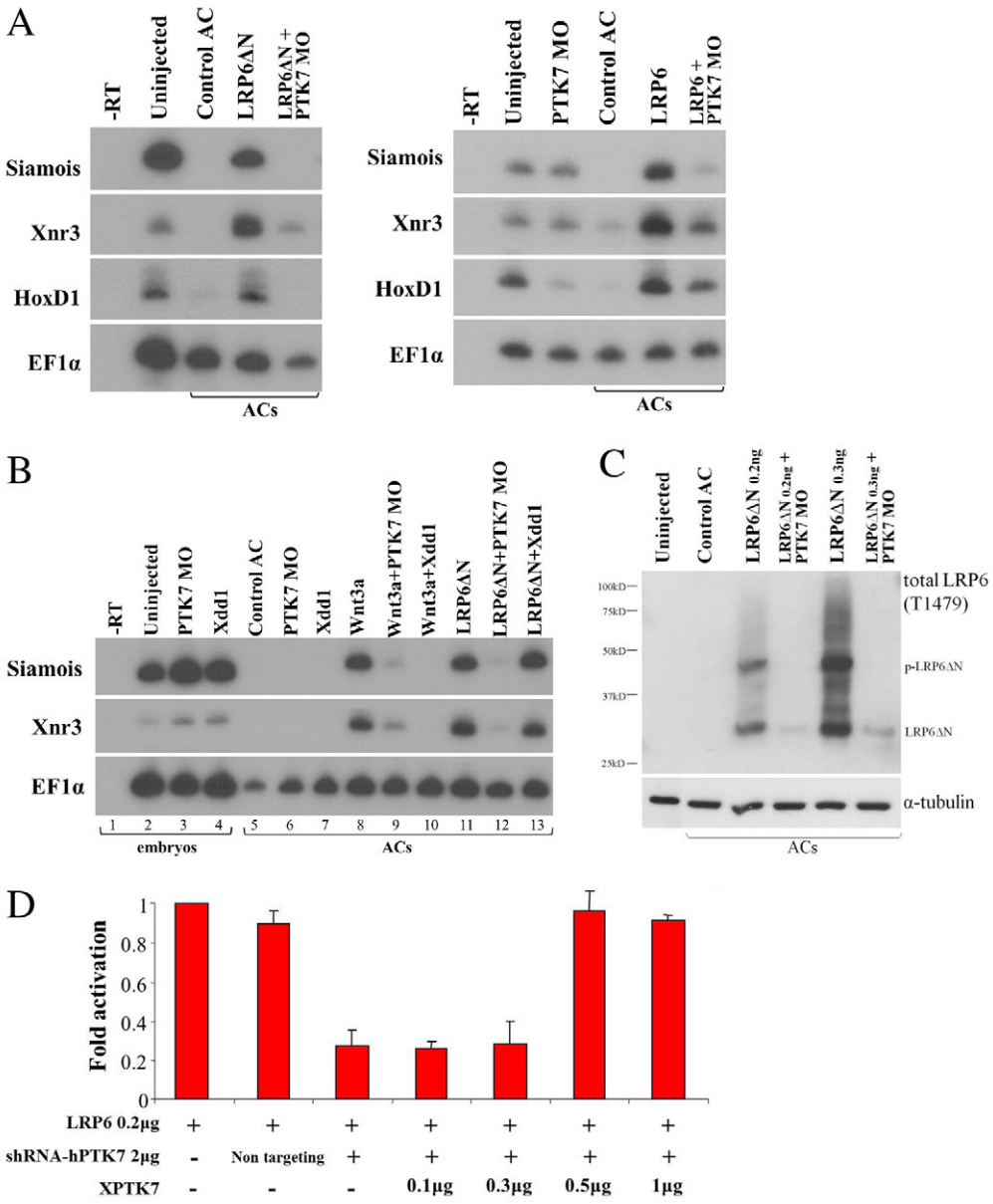

Fig. 3. PTK7 protein depletion inhibits LRP6 activity by reducing LRP6 protein levels. (A) Left panel: embryos were injected at the one-cell stage with *PTK7*-MO (10 ng) and RNA encoding the constitutively activated LRP6ΔN (170 pg) protein. ACs removed at the blastula stage were grown until gastrula st.10.5, when total RNA was isolated from six control embryos and 27 ACs from each group. Wnt direct-target gene expression was examined by sqRT-PCR. Right panel: embryos were injected at the one-cell stage with *PTK7*-MO (15 ng) and RNA encoding the full-length VSVG tagged LRP6 (2 ng) protein. ACs removed at the blastula stage were grown to gastrula st.10.5, when total RNA was isolated from six control and injected embryos and 27 AC explants from each group. Wnt direct-target gene expression was examined by sqRT-PCR. (B) Embryos were injected at the one-cell stage with RNA encoding the Wnt3a (5 pg, lanes 8-10) or LRP6ΔN (100 pg, lanes 11-13) proteins. These embryos were than co-injected with either the *PTK7*-MO (10 ng, lanes 6,9,12) or RNA encoding the dominant-negative Dvl protein (Xdd1, 0.7 ng, lanes 7,10,13). ACs removed at the blastula stage were grown to gastrula st.10.5, when total RNA was isolated from six control and injected embryos (lanes 2-4) and 18 ACs from each group. Wnt direct-target gene expression was examined by sqRT-PCR. (C) Embryos were injected at the one-cell stage with *PTK7*-MO (13 ng) and RNA encoding the constitutively activated LRP6ΔN (200 and 300 pg) protein. ACs removed at the blastula stage were grown to gastrula st.10.5. Total protein was isolated from 27 ACs per group for western analysis. The T1479 antibody recognizes unphosphorylated and phosphorylated forms of LRP6ΔN. (D) LRP6 induction of Wnt activity is PTK7 dependent. HEK293 cells were transfected with the *Topflash-luc* reporter, which was activated by co-transfection of LRP6 encoding DNA (0.2 μg). Co-transfection of a neutral *Renilla* vector serves as an internal control. A PTK7-targeting shRNA used to deplete endogenous PTK7 protein was compared with a nontargeting control shRNA. Increasing amounts of *Xenopus PTK7* encoding DNA were transfected as indicated. Data are presented as fold activation; the signal induced by LRP6 is presented as 1. Fold-activation from seven independent experiments is shown.

PTK7 maintains normal LRP6 protein levels: knockdown phenotypes are similar

To examine PTK7 modulation of normal LRP6 protein levels, experiments were performed with wild-type LRP6 protein. PTK7-depletion caused a sharp reduction of ectopically and endogenously expressed wild-type LRP6 protein levels (Fig. 4A,B). In PTK7 morphants, endogenous LRP6 protein levels resembled LRP6 morphants (Fig. 4B). To show *PTK7*-MO specificity, we performed

Development (2014) doi:10.1242/dev.095984

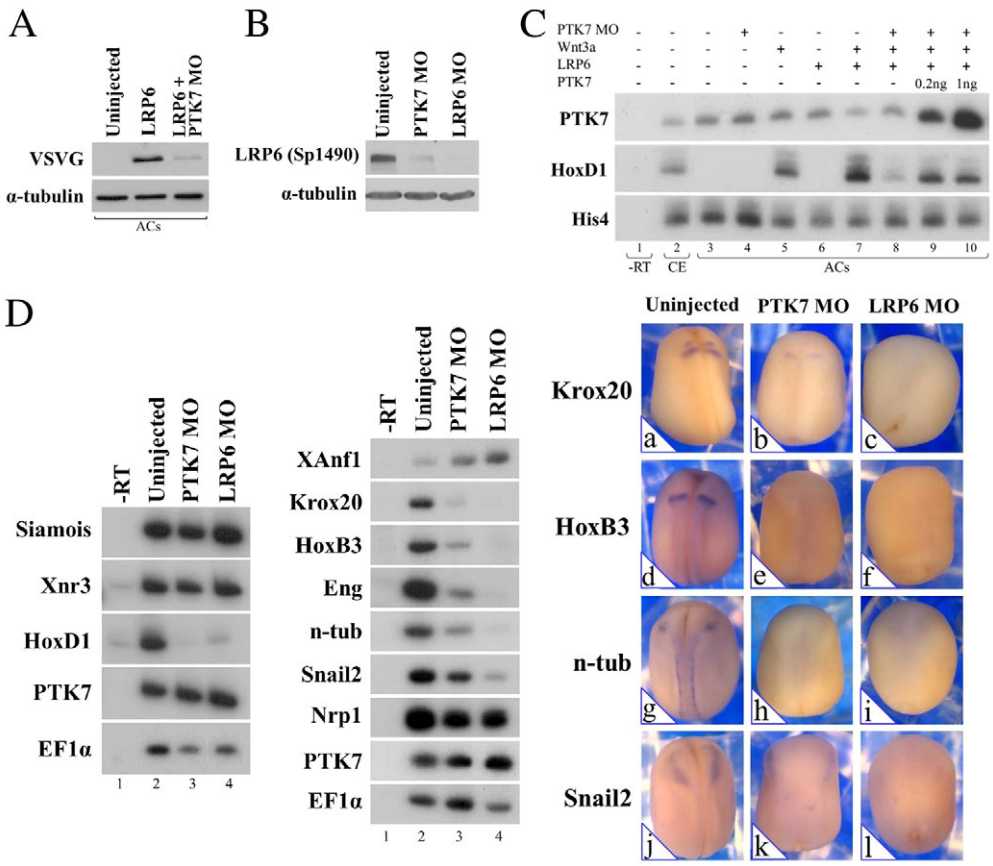

Fig. 4. PTK7 and LRP6 protein depletion gives identical phenotypes. (A) Embryos were injected at the one-cell stage with *PTK7*-MO (13 ng) and RNA encoding full-length tagged VSVG-LRP6 (1.5 ng) protein. ACs removed at the blastula stage were grown to gastrula st.10.5. Total protein was isolated from 18 ACs per group for western analysis. The VSVG antibody recognizes ectopically expressed LRP6 protein. (B) Embryos were injected at the one-cell stage with either the *PTK7*-MO (25 ng) or the *LRP6*-MO (25 ng). Embryos were grown to gastrula st.10.5. Total protein was isolated from ten embryos per group for western analysis. The Sp1490 antibody recognizes endogenous LRP6 protein. Whereas LRP6 protein levels were reduced, the *PTK7*-MO did not reduce *lrp6* mRNA levels (not shown). (C) Embryos were injected at the one-cell stage with the *PTK7*-MO (lanes 4,8-10) and RNA encoding the Wnt3a (5 pg, lanes 5,7-10) and full-length VSVG-LRP6 (0.5 ng, lanes 6-10) proteins. These embryos were than co-injected with increasing doses of PTK7-encoding RNA (0.2 ng, 1 ng; lanes 9,10). ACs removed at the blastula stage were grown to gastrula st.10.5, when total RNA was isolated from six control (lane 2) and 18 ACs from each group (lanes 3-10). *HoxD1* gene expression was measured by sqRT-PCR. *His4* and PTK7 gene expression are controls for loading and injection, respectively. (D) Left panel: sqRT-PCR to pools of six gastrula (st.10.5) embryos (lane 2) injected at the one-cell stage with *PTK7*-MO (10 ng, lane 3) or *LRP6*-MO (20 ng, lane 4). *Siamois*, *Xnr3* and *HoxD1* expression was compared in the morphants. PTK7 mRNA levels are unaltered by protein knockdown. Center panel: sqRT-PCR to pools of six neurula (st.17) sibling embryos shown in the left panel. *Nrp1* (pan-neural marker) and *PTK7* mRNA levels are unaltered by protein knockdown. Right panel: Embryos were injected at the one-cell stage with *PTK7*-MO (10 ng) or *LRP6*-MO (20 ng). Four posterior neural markers were analyzed by *in situ* hybridization. Neurula-stage embryos (st.17), viewed dorsally, anterior is on top. *Krox20* expression (a) is normal in 100% of the control embryos (n=10), perturbed (b) in 100% of the PTK7-morphant embryos (n=12) and (c) 100% of the LRP6 morphants (n=10). *HoxB3* expression (d) is normal in all of the controls (n=10) and perturbed (e) in 100% of the PTK7 morphants (n=11) and (f) 100% of the LRP6 morphants (n=10). *N-tub* expression is normal (g) in 82% of the controls (n=11), and perturbed (h) in 100% of the PTK7 morphants (n=12) and (i) 100% of the LRP6 morphants (n=10). *Snail2* expression is normal (j) in all controls (n=11) and perturbed (k) in 67% all of the PTK7 morphants (n=12) and (l) 100% of the LRP6 morphants (n=12).

an AC assay in which we co-injected Wnt3a with low levels of wild-type LRP6 protein (Fig. 4C). Co-injection of the *PTK7*-MO strongly inhibited Wnt3a/LRP6-induced *hoxd1* gene expression (Fig. 4C, lanes 7,8), yet co-expression of PTK7 protein partially rescued *hoxd1* levels (Fig. 4C, lanes 7-10). Under these conditions, ectopic PTK7 probably stabilizes some exogenous LRP6 protein, enabling *hoxd1* gene expression. Upon comparison, we found that the PTK7-morphant embryos phenocopy LRP6 morphants (Fig. 4D). LRP6 and PTK7 morphants both poorly express posterior neural markers at early/mid-neurula stages, but expression of the anterior forebrain marker, *xanf1* was increased (Fig. 4D). Pan-neural marker *nrp1* expression is not significantly reduced in either PTK7 or LRP6 morphants, versus controls (Fig. 4D, middle panel). Thus, neural patterning, but not neural induction is perturbed. Both morphant groups have similar morphology, poor neural tube folding, coupled to weak posterior neural marker expression (Fig. 4D, right panel), characteristic of embryos with reduced zygotic canonical Wnt or Meis3 activities.

LRP6 and PTK7 proteins inhibit Wnt-PCP activity in embryos

Studies in *Xenopus* showed that PCP inhibitors robustly rescue perturbed CE phenotypes induced by excess expression of PCP-activating components (Djiane et al., 2000; Penzo-Mendèz et al., 2003). This assay can determine if a specific protein is an inhibitor or activator of the PCP pathway. In this assay, LRP6 protein was a PCP inhibitor; ectopic LRP6 rescued CE in explants co-expressing

Development (2014) doi:10.1242/dev.095984

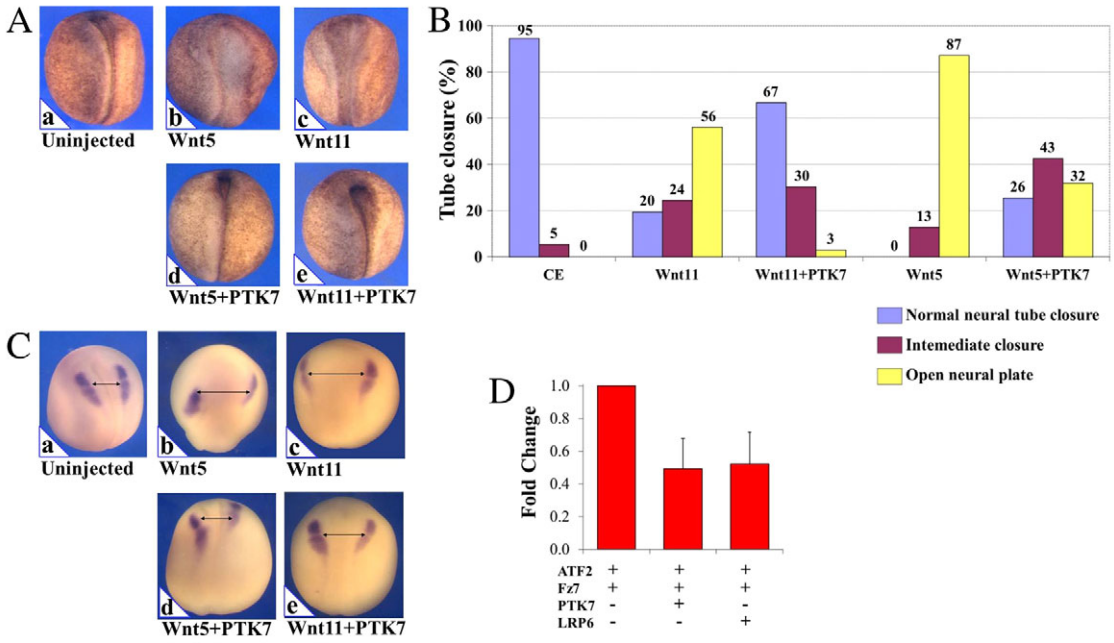

Fig. 5. PTK7 inhibits Wnt-PCP activity in *Xenopus* embryos. (A) PTK7 inhibits excess Wnt-PCP activity to rescue neural folds closure. Embryos were injected animally at the one-cell stage with RNA encoding Wnt5 (250 pg) or Wnt11 (350 pg) (b,c). To rescue neural folding, *ptk7* (200 pg) mRNA was co-injected (d,e). Neurula-stage embryos are viewed dorsally (a); anterior is on top. Neural folds closure is increased in the PTK7 co-expressing embryos (d,e) versus the Wnt5- or Wnt11-expressing embryos (b,c). (B) Statistics of the experiment shown in Fig. 5A. Embryos were scored as having a completely open neural plate (yellow), intermediate neural plate folding (purple) or normal folding (blue). In control embryos (CE, *n*=55), 95% of the embryos had normal neural folds. In Wnt11-expressing embryos (*n*=41), 20% had normal neural folds and 56% had an open neural plate; by contrast, in the Wnt11/PTK7-expressing embryos (*n*=33), 67% had normal neural folds, and only 3% had an open neural plate. In Wnt5-expressing embryos (*n*=39), no embryos had normal neural folds and 87% had an open neural plate; by contrast, in the Wnt5/PTK7-expressing embryos (*n*=47), 26% had normal neural folds, and only 32% had an open neural plate. This is one representative experiment of three repeats. (C) *snail2* expression patterns detect the distance between the neural folds in Wnt5±PTK7 and Wnt11±PTK7 co-expressing embryos. Embryos (a) were injected as described in Fig. 5A. *snail2* expression was analyzed at the neurula stage. The arrowheads mark the distance between the inner edges of the neural folds. Note the differences in b versus d (Wnt5±PTK7) and c versus e (Wnt11±PTK7). (D) Embryos at the one-cell stage were injected with 75 pg of the *ATF2-luciferase* reporter vector and *Fz7* (400 pg), in combination with either *ptk7* (200 pg) or *lrp6* (300 pg) mRNA. The control (ATF2-luc + Fz7) is set as 1. In each experiment a pool of 12 early neurula-stage embryos from each injected group were assayed for luc activity. Luc activity was normalized to protein levels in each group. This graph represents a pool of six independent experiments.

high Wnt11 levels, by inhibiting excess PCP activity (Tahinci et al., 2007; Bryja et al., 2009).

We used this strategy to address whether PTK7 inhibits Wnt-PCP activity regulating neural plate folding. Excess Wnt11 or Wnt5 expression strongly inhibited neural plate closure (compare Fig. 5Aa-c). Co-expression of PTK7 strongly rescued this perturbation phenotype (compare Fig. 5Ab,c and 5Ad,e). Control embryos had normal neural plate closure (95%), versus Wnt11-injected (20%) and Wnt5-injected (0%) embryos (Fig. 5B). Reciprocally, there was a robust perturbed open neural plate phenotype in Wnt11-expressing (56%) and Wnt5-expressing (87%) embryos (Fig. 5B). PTK7 strongly rescued neural plate closure defects in Wnt11 (67% normal, 30% partial, *n*=33) and Wnt5 (26% normal, 43% partial, *n*=47) co-expressing embryos (Fig. 5B). The ratio of 'completely' open neural plates was reduced nearly 20-fold in the PTK7/Wnt11 rescue group and nearly threefold in the PTK7/Wnt5 group versus the non-PTK7 expressing sibling embryos (Fig. 5B). Ectopic Wnt5 gave a stronger phenotype than Wnt11, and was thus harder to rescue (Fig. 5B). Like PTK7, LRP6 also rescued neural plate closure (not shown).

Additionally, the distance between the neural crest-specific *snail2* expression domains at neurula stage (st.) 16-17 is used to measure the width of the neural plate, being diagnostic for reduced CE. Ectopic Wnt5/11 expression expands this distance (compare Fig. 5Ca and 5Cb,c), which was significantly reduced by PTK7 co-expression (Fig. 5Cd,e). These experiments show that PTK7 expression robustly rescues neural plate CE and folding perturbations triggered by excess Wnt-PCP activity, strong proof that PTK7 acts to antagonize and not enhance Wnt-PCP activity.

In *Xenopus* embryos, the *ATF2-luc* reporter plasmid is a readout for Wnt-PCP activity, being activated by co-expression with Fz7, Wnt5a or Wnt11 proteins (Ohkawara and Niehrs, 2011). We activated this reporter with Fz7, and then co-expressed ectopic levels of either PTK7 or LRP6 protein (Fig. 5D). Both proteins similarly inhibited Fz7 induction of the reporter (Fig. 5D). Under similar experimental conditions to the reporter assay, PTK7 also rescues the open neural plate phenotype induced by ectopic Fz7 expression. Fz7 expression induces open neural plates in 47% (*n*=100) of the injected embryos versus 11% of the controls (*n*=132), whereas PTK7 overexpression reduces open neural plates by over fourfold, returning levels to 11%, like the controls (*n*=72; three independent experiments). Also, in embryos in which Fz7/Wnt5 proteins are co-expressed at lower additive concentrations to perturb neural plate closure, ectopic PTK7 strongly rescues neural folding, while also inhibiting the PCP-reporter assay (not shown).

We also performed experiments similar to those described for LRP6 rescue of excess Wnt11 inhibition of activin-induced CE in ACs (Tahinci et al., 2007). We compared CE in ACs co-expressing the

Development (2014) doi:10.1242/dev.095984

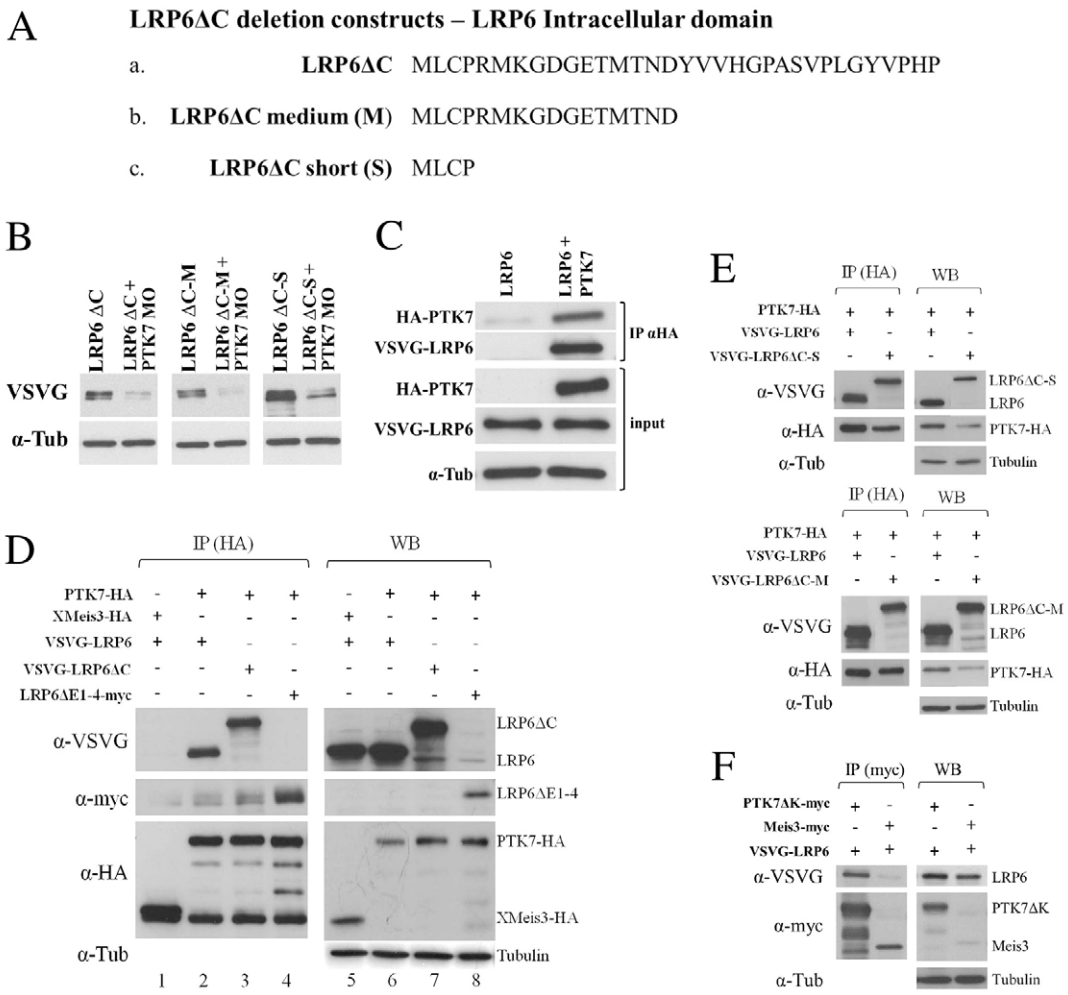

Fig. 6. PTK7 and LRP6 proteins physically interact. (A) LRP6ΔC deletion constructs. The intracellular amino acid residues for each construct (a-c) are shown. (B) Embryos were separately injected at the one-cell stage with RNA (2 ng) encoding the VSVG-tagged LRP6ΔC, LRP6ΔC-M or LRP6ΔC-S proteins and *PTK7*-MO (10 ng). Embryos were grown to gastrula st.10. Total protein was isolated from 27 ACs per group for western analysis using the VSVG antibody. (C) Embryos were co-injected at the one-cell stage with RNA (2 ng) encoding VSVG-LRP6 and PTK7-HA proteins. Embryos were grown to early-neurula st.12. Total protein was isolated from 25 embryos per group for IP and western analysis. IP was done by anti-HA antibody (targeting PTK7 protein) on protein A-Sepharose beads. The co-IP proteins were blotted with VSVG and HA antibodies. (D) HEK293 cells were transfected with the PTK7-HA, VSVG-LRP6, VSVG-LRP6ΔC and LRP6ΔE1-4-myc expression plasmids (lanes 2-4). Whole-cell extracts were immunoprecipitated by HA antibody (targeting PTK7 protein) on protein G Agarose beads. The co-IP proteins were blotted with VSVG, myc and HA antibodies. Cells transfected with Meis3-HA were an HA-tag control (lane 1). The left panel shows the immunoprecipitated proteins and the right panel shows total protein expression input. (E) HEK293 cells were transfected with the PTK7-HA, VSVG-LRP6 and the VSVG-LRP6ΔC-S (upper panel) or LRP6ΔC-M (lower panel) expression plasmids as indicated. Co-IP was performed as described in D. The co-IP proteins were detected by VSVG and HA antibodies. The left and right panel as described in D. (F) HEK293 cells were transfected with the PTK7ΔK-myc and the LRP6-VSVG expression plasmids. Whole-cell extracts were prepared and immunoprecipitated with the myc antibody, targeting PTK7ΔK protein. The co-IP proteins were detected by VSVG and myc antibodies. Cells transfected with Meis3-myc are the tag control. The left and right panel as described in D.

activated-activin receptor, Alk4 + Wnt11 and either LRP6 or PTK7 proteins (supplementary material Fig. S1). PTK7 or LRP6 co-expression both strongly rescued Wnt11 inhibition of mesodermal CE in AC explants, whereas the *PTK7*-MO enhances CE perturbation by Wnt11 (supplementary material Fig. S1). These results show that PTK7, like LRP6 protein, negatively modulates Wnt-PCP activity.

LRP6 and PTK7 proteins inhibit Wnt-PCP activity in cultured cells

Ultraviolet (UV) irradiation induces JNK-activation and phosphorylation of c-Jun in cultured HEK293 cells (Weidenfeld-Baranboim et al., 2011). Wnt-PCP pathway components also efficiently induce c-Jun phosphorylation (Funato et al., 2008). To determine if LRP6 or PTK7 inhibits endogenous c-Jun phosphorylation, these proteins were transfected into HEK293 cells that were UV irradiated. Expression of dominant-negative PCP-inhibitory Wnt11 and Fzl7 proteins (supplementary material Fig. S2A), or PTK7 and LRP6 proteins (supplementary material Fig. S2B) severely reduced UV-induced c-jun phosphorylation. Thus, LRP6 and PTK7 proteins act as inhibitors and not activators of Wnt-PCP dependent JNK-activation.

PTK7 and LRP6 proteins physically interact

To identify a PTK7 interacting domain in the cytoplasmic region, we systematically deleted the LRP6 protein intracellular domain. The LRP6ΔC protein has 33 amino acids of intracellular region

Development (2014) doi:10.1242/dev.095984

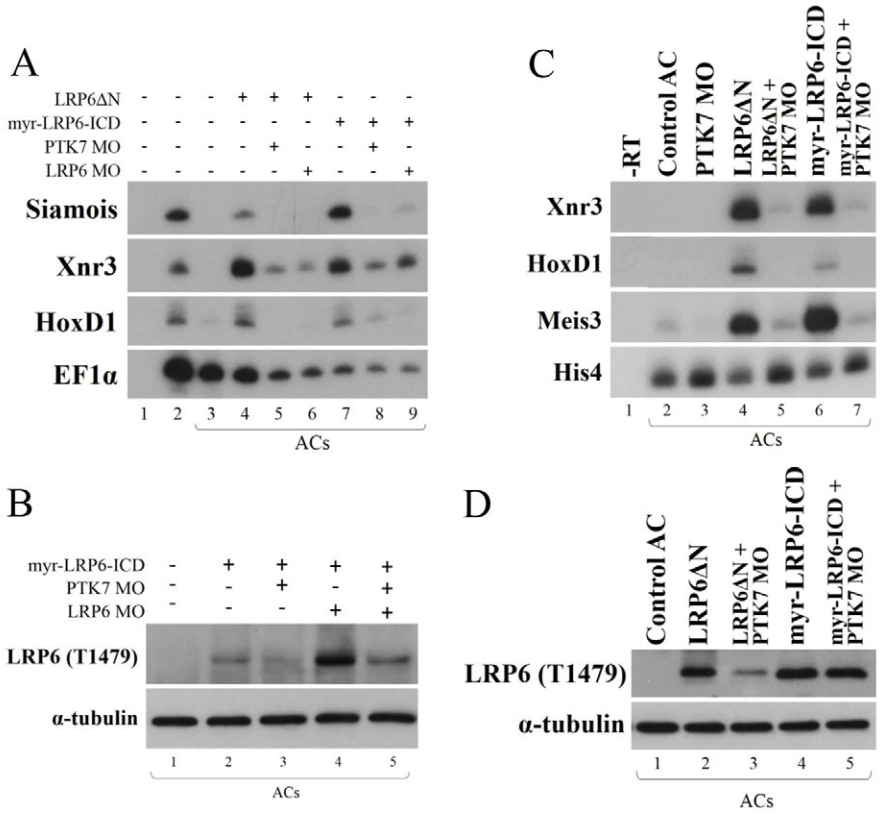

Fig. 7. Constitutively activated LRP6 proteins interact with endogenous LRP6 protein. (A) Embryos were injected at the one-cell stage with RNA encoding LRP6ΔN (170 pg) or myr-LRP6-ICD (500 pg) proteins (constitutively activated constructs) and the *PTK7*-MO (10 ng) or *LRP6*-MO (10 ng). AC explants were removed from control and injected embryos at blastula stage and grown to gastrula st.10.5. Total RNA was isolated from six control embryos and 27 ACs from each group. Wnt direct-target gene expression was examined by sqRT-PCR. (B) Embryos were injected at the one-cell stage with *myr-LRP6-ICD* mRNA (1 ng) and the *PTK7*-MO (10 ng), *LRP6*-MO (20 ng) or both. ACs removed at the blastula stage were grown to gastrula st.10.5. Total protein was isolated from 27 ACs per group for western analysis using the anti-LRP6 T1479 antibody. (C) Embryos were injected at the one-cell stage with RNA encoding LRP6ΔN (100 pg) or myr-LRP6-ICD (400 pg) proteins and the *PTK7*-MO (13 ng). ACs were cultured as described, and lysis was performed on 36 pooled explants per AC group for sqRT-PCR. Wnt direct-target gene expression was examined by sqRT-PCR. (D) Duplicate western analysis of the experiment described in C. For western analysis, the T1479 antibody recognizes LRP6ΔN and myr-LRP6-ICD proteins.

starting with MLCP amino acid residues following the transmembrane domain (Fig. 6A). The LRP6ΔC protein was further deleted to constructs having only 16 (LRP6ΔC-M), and four (LRP6ΔC-S) intracellular domain amino acid residues (Fig. 6A). These truncated LRP6 proteins were all unstable in the absence of PTK7 protein (Fig. 6B). This instability suggests that the LRP6 intracellular domain may not be interacting with the PTK7 protein solely through these motifs. To address PTK7/LRP6 protein-protein interactions, co-immunoprecipitation (co-IP) assays were performed in *Xenopus* embryos and HEK293 cells. In both *Xenopus* and HEK293 cells, full-length PTK7 and LRP6 proteins physically interact, undergoing co-IP (Fig. 6C,D lanes 1,2). In HEK293 cells, activated LRP6ΔE1-4 and LRP6ΔC, LRP6ΔC-M and LRP6ΔC-S truncated constructs all co-IP with PTK7 protein (Fig. 6D,E). The various LRP6 constructs lacking nearly all of the extracellular (LRP6ΔN, LRP6ΔE1-4) or intracellular domains (LRP6ΔC-S) were unstable in the absence of PTK7 protein (Fig. 3C; Fig. 6B) and all co-IP with wild-type PTK7 protein (Fig. 6D,E). The intracellular truncated dominant-negative PTK7ΔK protein also co-immunoprecipitates with wild-type LRP6 protein (Fig. 6F). By contrast, The CK1-γ and GSK3β components of the LRP6-signalosome complex do not co-immunoprecipitate with wild-type PTK7 protein in HEK293 cells (not shown).

Constitutively activated LRP6 proteins require endogenous LRP6 protein

Like LRP6ΔN/LRP6EΔ1-4, the mouse myr-LRP6-ICD is a constitutively activated protein that has a complete intracellular domain, but the LRP6 transmembrane domain has been swapped to an N-terminal myristoylation target sequence (Cselenyi et al., 2008). LRP6ΔN or myr-LRP6-ICD induction of Wnt target genes was inhibited by PTK7 knockdown (Fig. 7A, lanes 4,5,7,8). When myr-LRP6-ICD is expressed in PTK7-morphant ACs, it appears somewhat more stable than other mutant LRP6 proteins, as levels are highly variable between experiments (compare Fig. 7B, lanes 2,3 and 7D, lanes 4,5), suggesting that additional regions outside the membrane domain may also function in protein stability. Regardless of myr-LRP6-ICD protein levels, its induction of Wnt target gene expression was strongly inhibited by PTK7 depletion (Fig. 7A,C). Similar to PTK7 depletion, the LRP6ΔN and myr-LRP6-ICD protein activities were both also inhibited identically by endogenous LRP6 protein depletion (Fig. 7A), suggesting a requirement for interaction with the endogenous LRP6 protein. In support, we found that the constitutively activated truncated LRP6 proteins co-immunoprecipitates with wild-type LRP6 protein in HEK293 cells (supplementary material Fig. S3). Surprisingly, the *LRP6*-MO not only inhibits Wnt target gene activity by myr-LRP6-ICD, but also

Development (2014) doi:10.1242/dev.095984

elevates myr-LRP6-ICD protein levels, in contrast to the *PTK7*-MO, which lowers them (Fig. 7B). These results give novel insights into the activity mechanism of constitutively activated LRP6 proteins, demonstrating their dependence on endogenous wild-type LRP6 protein for activity and degradation. Wnt cascade activation enhances LRP6 degradation (Li et al., 2010), and myr-LRP6-ICD protein associated with endogenous LRP6 appears to be degraded. After LRP6 protein depletion and signalosome loss, inactive myr-LRP6-ICD protein 'alone' in the membrane is more stable (Fig. 7B), undergoing slower turnover.

DISCUSSION

Canonical and noncanonical PCP-Wnt signaling pathways regulate cell morphogenesis and cell fate in different systems (Wallingford et al., 2002; Elkouby and Frank, 2010). The canonical and noncanonical Wnt pathways also mutually interact. PCP signaling inhibited canonical activity (Kühl et al., 2001; Yan et al., 2001; Saneyoshi et al., 2002), whereas the canonical Wnt antagonist Dkk1 protein stimulated PCP activity (Caneparo et al., 2007). During both *Xenopus* and mouse development, high LRP6 protein levels suppress Wnt-PCP activity, whereas LRP6 protein knockdown activates high Wnt-PCP activity, blocking CE movements in explants (Tahinci et al., 2007; Bryja et al., 2009). LRP6 protein seems to balance optimal canonical versus PCP Wnt signaling levels.

Neural expressed *meis3* is a direct target of mesodermal Wnt3a signaling, and Meis3 protein acts downstream to specify posterior neural cell fates, inducing Wnt-PCP dependent CE (Elkouby et al., 2010; Aamar and Frank, 2004). PTK7 protein regulates CE movements in both mouse and *Xenopus* embryos (Lu et al., 2004; Yen et al., 2009; Paudyal et al., 2010). PTK7 is expressed in the *Xenopus* neural plate; its knockdown impairs neural CE (Lu et al., 2004). We speculated that PTK7 is positioned downstream of Meis3 protein to regulate neural CE. However, Meis3/PTK7 epistasis experiments showed that *ptk7* gene expression is normal in Meis3 morphants, but *meis3* expression is severely inhibited in PTK7 morphants. Moreover, PTK7 knockdown embryos phenocopy Wnt loss-of-function and Meis3-morphant phenotypes. Besides inhibited neural CE, PTK7 knockdown causes a broader loss of posterior neural cell fates, including hindbrain, neural crest and primary neurons. In *Xenopus*, the PTK7-morphant phenotype is zygotic and not maternal, as expression of maternally regulated Wnt direct-target genes such as *xnr3* and *siamois* is never inhibited, whereas expression of early zygotic Wnt direct-target genes, such as *meis3* and *hoxd1*, is severely inhibited.

As PTK7 is a transmembrane protein acting zygotically upstream of Meis3, we speculated that PTK7 regulated Wnt signaling via ligands or receptors. Indeed, in AC assays, PTK7 protein knockdown inhibited Wnt pathway activation, as measured by target-gene marker expression, when either Wnt ligands or LRP6 proteins were ectopically expressed. We found that LRP6 protein levels are severely reduced in PTK7-morphant embryos or explants. Canonical Wnt signaling is highly compromised by this loss of LRP6 protein levels. Indeed, PTK7 morphants identically phenocopied LRP6 morphants; embryos and explants lose posterior neural cell fates and do not undergo proper neural CE.

Assessing Wnt-PCP levels in CE assays is complex, because the depletion or excess of Wnt-PCP is incompatible with CE (Wallingford et al., 2000; Djiane et al., 2000). Opposite effectors give similar outputs. When activin induces CE in ACs, ectopic Wnt11 protein blocks it. In these ACs, co-expression of Wnt-PCP pathway inhibitors rescues CE by reducing overwhelmingly excess PCP levels (Djiane et al., 2000). CE in Keller explants and ACs was rescued by excess LRP6 levels, canceling out PCP overstimulation by Wnt11. Thus, LRP6 protein represses Wnt-PCP activity; reciprocally, LRP6 depletion overstimulates Wnt-PCP activity, inhibiting CE (Tahinci et al., 2007; Bryja et al., 2009).

We show in embryos, explants and cultured cells that PTK7, like LRP6, acts as a Wnt-PCP inhibitor. Both proteins rescue neural plate CE and folding inhibited by ectopic Wnt5, Wnt11 or Fz7 expression that overstimulates PCP. In ACs, we show that PTK7, similar to LRP6, rescues activin-induced CE inhibited by PCP overstimulation. Studies suggested that PTK7 protein is required for embryo morphogenesis to positively modulate Wnt-PCP activity (Lu et al., 2004; Shnitsar and Borchers, 2008; Hayes et al., 2013). We suggest that during *Xenopus* development, PTK7 stabilization of LRP6 protein negatively modulates Wnt-PCP activity. The reduction of LRP6 protein levels via the *LRP6*-MO or via *PTK7*-MO triggers an increase in Wnt-PCP signaling that inhibits CE.

Both LRP6 and PTK7 are transmembrane proteins. In co-IP assays, these proteins physically interact in both *Xenopus* and human cells. Deletion of the entire LRP6 intracellular domain does not inhibit PTK7 binding. LRP6 proteins lacking the extracellular domain also co-immunoprecipitate with PTK7, suggesting that PTK7 and LRP6 proteins interact via their transmembrane domains. PTK7 also binds dominant-negative LRP6 protein; thus LRP6 protein need not be engaged in Wnt signaling to bind PTK7. LRP6 protein is the gatekeeper of the canonical Wnt pathway. Components that activate β-catenin/Wnt signaling, such as Wnts and Dvl all require functional Fz/LRP6 receptor complexes; these proteins cannot induce Wnt target gene transcription in the absence of PTK7 or LRP6 proteins. In either PTK7- or LRP6-morphant cells, we suggest that the Wnt ligand fails to signal, Dvl cannot form signalosomes and β-catenin protein will be less stable.

Recent studies in *Xenopus* and zebrafish concluded differently concerning the interactions between PTK7 and canonical Wnt signaling (Puppo et al., 2011; Peradziryi et al., 2011; Hayes et al., 2013). One *Xenopus* study suggests that PTK7 is required for canonical Wnt signaling and PTK7 knockdown blocks maternal Wnt target gene expression in embryos (Puppo et al., 2011). The initial activation of Spemann organizer-specific genes is dependent on intracellular Wnt signaling components. Maternal Wnt 5a/11 proteins regulate organizer formation (Cha et al., 2008). Only by MO depletion of maternal Wnt pathway components in oocytes are organizer ablation phenotypes observed (Heasman et al., 2000; Kofron et al., 2007). Our results show that PTK7 and LRP6 protein depletion does not affect organizer formation; maternally regulated *xnr3* and *siamois* gene expression is not reduced in PTK7- or LRP6-morphant embryos, whereas expression of the zygotic direct Wnt target genes *hoxd1* and *meis3* is severely repressed. Furthermore, *PTK7*-MO injected embryos had phenotypes resembling zygotic Wnt loss of function. Our neural phenotype resembles embryos described in other PTK7 protein knockdown studies in *Xenopus* (Lu et al., 2004). PTK7 morphants do not resemble β-catenin knockdown embryo phenotypes, in which the body axis is severely perturbed and *xnr3* and *siamois* gene expression is lost (Heasman et al., 2000). Our present work and similar studies utilize simultaneous co-injection of two *PTK7*-MOs at relatively low concentrations (Shnitsar and Borchers, 2008). The organizer phenotype study used different *PTK7*-MOs, at a fourfold higher concentration per/blastomere (Puppo et al., 2011). This variation in MO strategies might explain the differences in their observed phenotypes, which resemble maternal LRP6 depletion (Kofron et al., 2007). In zebrafish, maternal PTK7 knockdown was performed (Hayes et al.,

Development (2014) doi:10.1242/dev.095984

2013). In contrast to the zygotic *Xenopus* phenotype (Lu et al., 2004), the maternal zebrafish phenotype has a more profound effect on mesodermal CE versus neural CE. There are a few possibilities to explain potentially different PTK7 function and phenotypes between species and embryonic stages. Studies in cancer cells have uncovered five unique proteolytic fragments of PTK7, in addition to the full-length protein. These PTK7 isoforms differ in both subcellular localization and apparent function (Golubkov and Strongin, 2012; Na et al., 2012). These PTK7 isoforms could differentially regulate canonical or noncanonical Wnt activities in a cell-context-specific manner. Unraveling the mechanistic function of other PCP components during development has also been difficult. Like PTK7, Frd1/2-Dapper proteins also gave conflicting results as to their role regulating canonical and noncanonical Wnt signaling, especially in overexpression assays (reviewed by Brott and Sokol, 2005). Determining the cellular mechanism by which Vangl2/Pk1 overexpression or knockdown modulates PCP has also been elusive (reviewed by Roszko et al., 2009). Further studies in different model systems should clarify these points.

Other studies suggest that PTK7 protein inhibits canonical Wnt signaling by interacting with Wnt ligands (Peradziryi et al., 2011; Hayes et al., 2013). These studies are mainly based on ectopic PTK7 expression and inhibition of Wnt-activated reporter constructs. Our study mainly utilizes PTK7 protein knockdown. Identifying LRP6 as the nexus of PTK7 protein activity is a key discovery in our experiments. In many systems, ectopic gene expression will give phenotypes resembling gene knockdown phenotypes. Ectopic excess PTK7 protein levels above a threshold could titrate out Wnt or LRP6 proteins from normal complexes, disrupting canonical Wnt signaling, not necessarily recapitulating endogenous physiological function. We demonstrate that PTK7-morphant embryo phenotypes resemble canonical Wnt knockdowns, supporting our data showing LRP6 protein depletion. These observations do not support the idea that PTK7 protein inhibits canonical Wnt signaling. If PTK7 acted as a canonical Wnt inhibitor, we would not expect it to rescue posterior neural marker gene expression. We would also not expect that ectopic PTK7 would rescue of neural folding, nor not inhibit expression of the *snail2* neural crest marker, as *snail2* expression is extremely sensitive to the loss of canonical Wnt signaling.

In *Xenopus*, ectopically expressed PTK7 mediated Dvl and RACK membrane recruitment during PCP (Shnitsar and Borchers, 2008; Wehner et al., 2011). These results differ from those in mouse and zebrafish, in which *Ptk7* knockout mice and zebrafish show no genetic interactions with, or disruptions of, endogenous Dvl protein localization, despite having strong PCP phenotypes (Yen et al., 2009; Lee et al., 2012; Hayes et al., 2013). The *Xenopus* studies do not examine endogenous protein. This same *Xenopus* study also claims that the *PTK7*-MO blocks neural CE in ACs induced by ectopic FoxD1 (XBF-2) protein. This experiment does not determine if the *PTK7*-MO blocks canonical Wnt caudalizing activity, preventing neural caudalization and CE by FoxD1 in ACs (Fonar et al., 2011).

In mouse auditory epithelium morphogenesis, PCP activity is required for the apical formation of stereociliary bundles in sensory hair cells (Lee et al., 2012). In mice, *Ptk7* or the noncanonical *Fz3/Fz6* receptor knockouts give a similar PCP-phenotype; hair cell bundle misorientation is accompanied by a loss of vinculin planar asymmetry. However, in double homozygous mutants of *Ptk7/Fz3* or *Ptk7/Fz6*, bundle orientation and vinculin asymmetry are restored (Lee et al., 2012). Ptk7 and Fz3/6 proteins act in an apparent antagonist manner to control epithelial cell PCP. These results strongly support our observations in *Xenopus* that PTK7 acts to restrain PCP during neural CE.

A fine-tuned balance of canonical and PCP activities is essential for correct nervous system development. In *Xenopus*, canonical Wnt activity initially induces posterior fates; these cells then undergo neural CE movements via activation of the Wnt-PCP pathway. Thus, early inhibition of canonical Wnt activity prevents later neural CE by eliminating posterior neural cell fates. Also, LRP6 and PTK7 proteins positively modulate canonical activity, while simultaneously inhibiting noncanonical PCP activity to fine-tune optimal Wnt signaling levels (Tahinci et al., 2007; Bryja et al., 2009). These two LRP6/PTK7-requiring functions, neural fate specification and Wnt-PCP inhibition, are not necessarily mutually exclusive. Earliest induction of posterior neural cell fates may initially require a higher canonical to PCP activity ratio, whereas later, during CE movements, this balance may shift to favor PCP activity. At later stages, *wnt3a* is expressed locally and not ubiquitously in the neural plate (Fonar et al., 2011). In the absence of canonical Wnt signaling, ectopic expression of the Meis3 protein robustly induces neural marker expression and CE (Elkouby et al., 2010; Elkouby et al., 2012), suggesting that after posterior neural specification, canonical Wnt activity is reduced to lower levels, permissive for neural CE.

PTK7 protein binds the LRP6 protein and is crucial for maintaining its stability. PTK7 knockdown depletes LRP6 protein levels crucial for activating caudalizing transcription factor targets, such as *meis3* and *hoxd1*. PTK7 and LRP6 protein knockdown both cause similar phenotypes; posterior neural cell fates and resultant neural CE are both lost. Both PTK7 and LRP6 proteins inhibit Wnt-PCP signaling when in excess. These findings suggest an exciting new role for PTK7. PTK7 regulates LRP6 protein levels, which maintain the canonical/PCP Wnt activity ratio, thus controlling posterior neural cell fate specification. Defects in both canonical and noncanonical Wnt signaling are linked to cancer, as are modulations in LRP6 and PTK7 protein activities (MacDonald et al., 2009; Wang, 2009; Golubkov and Strongin, 2012). Future experiments should determine if disrupted PTK7/LRP6 interactions modulating Wnt-network signaling play a functional role during carcinogenesis.

MATERIALS AND METHODS

Xenopus embryos

Ovulation, *in vitro* fertilization, culture and explant dissections were as described (Re'em-Kalma et al., 1995).

RNA and MO injections and plasmid constructs

Capped *in vitro* transcribed mRNA constructs of *ptk*7, *ptk7ΔK*, *huPTK7* (Shnitsar and Borchers, 2008); *meis3*, *noggin*, *wnt3a* (Elkouby et al., 2010); *dvl*, *dd1*, *wnt11* (Aamar and Frank, 2004), *activated-alk4 receptor* (R. Harland Lab); *lrp6*, *lrp6ΔN*, *lrp6ΔC*, *lrp6ΔE1-4* (Bilic et al., 2007; Zeng et al., 2008) were injected into one- or two-cell-stage embryos. Antisense MOs (Gene Tools): *Meis3*-MO, *PTK7*-MO, *LRP6*-MO (Dibner et al., 2001; Lu et al., 2004; Tahinci et al., 2007). Two-mixed *PTK7*-MOs were injected (Lu et al., 2004). The LRP6ΔC deletion constructs were deleted from the intracellular carboxy-end with two different 3′ end polymerase chain reaction (PCR) primers yielding constructs with 16 (LRP6ΔC-M) or four (LRP6ΔC-S) amino acid residues of the intracellular domain.

In situ hybridization

Whole-mount *in situ* hybridization was performed with digoxigenin-labeled probes: *krox20*, *hoxB3*, *n-tubulin* (*n-tub*) and *snail2* (Gutkovich et al., 2010).

Semi-quantitative reverse transcription (sqRT) PCR analysis

sqRT-PCR was performed (Snir et al., 2006). In all sqRT-PCR experiments, three to six independent experimental repeats were performed. Samples are

assayed at least twice for each marker. sqRT-PCR primers: *ef1a*, *his4*, *hoxD1*, *krox20*, *hoxB9*, *hoxB3*, *hoxB4*, *foxd3*, *n-tub* (Gutkovich et al., 2010); *siamois* and *xnr3* primer sequences (R. Harland Lab database). *Xenopus ptk7* primers: A: 5′-TACCGTGTGACCAATGAGGA-3′; B: 5′-CATGCCTC-CTAGCCTTTCTG-3′.

Cell culture and transfection

Human embryonic kidney cells (HEK293), were grown in Dulbecco's modified Eagle medium, fetal calf serum, glutamine and antibiotics. Cells were transfected by the calcium phosphate procedure.

Immunoprecipitation (IP) in *Xenopus* and HEK293 cells

RNAs (2 ng) encoding PTK7-HA and VSVG-LRP6 proteins were co-injected into one-cell-stage embryos. Twenty-five st.12 embryos from each group were lysed in hypotonic buffer. Lysates were centrifuged three times at 13,000 rpm. Protein A-Sepharose beads (Sigma) were washed three times with lysis buffer. Anti-HA antibody (Covance) was added to beads and rocked for 2 hours, at 4°C. Beads were rewashed and lysates were added. Rocking continued overnight, at 4°C. Beads were washed three times in lysis buffer + Triton 0.1%. Electrophoresis loading buffer was added. Proteins were detected by anti-HA and anti-VSVG antibodies. HEK293 cells were lysed on ice, 48 hours after transfection, with 500 µl IP buffer. Cells were vortexed for 10 seconds, every 5 minutes, for 15 minutes. Supernatant was collected after spinning the tubes at 10,000 rpm, for 15 minutes. For IP, the relevant antibody was added to the lysates and rocked for 1 hour, at 4°C; recombinant protein G-Agarose beads (Invitrogen) were added and rocked overnight. Beads were spun down for 5 minutes at 2500 rpm, and washed four times with IP buffer. Electrophoresis loading buffer was added.

Western analysis

Western analysis was performed as previously described (Zetser et al., 2001). Antibodies used were: LRP6-T1479 (1 µg/ml), LRP6-Sp1490 (1 µg/ml), α-Tubulin (Sigma T9026; mouse, 1:10,000), VSVG (Sigma V4888; rabbit, 1:2000), HA (Covance MMS101R; mouse, 1:1000), myc (Santa Cruz SC-789; rabbit, 1:1000). Secondary antibodies: goat anti-mouse (Thermo Scientific 31432; 1:4000), or goat anti-rabbit (Thermo Scientific 31460; 1:4000). α-Tubulin is the protein loading control.

Acknowledgements

We thank Drs A. Borchers, C. Niehrs, X. He, R. Harland and E. Lee for plasmids and antibodies.

Competing interests

The authors declare no competing financial interests.

Author contributions

N.B.-N., H.L., A.M. and D.F. designed the project, carried out experiments, analyzed data and wrote the paper. M.L. and S.E. designed and performed experiments and analyzed data.

Funding

D.F. was supported by grants from the Israel-Niedersachsen Fund [ZN2319] and the Israel Science Foundation [658/09].

Supplementary material

Supplementary material available online at
http://dev.biologists.org/lookup/suppl/doi:10.1242/dev.095984/-/DC1

References

Aamar, E. and Frank, D. (2004). Xenopus Meis3 protein forms a hindbrain-inducing center by activating FGF/MAP kinase and PCP pathways. *Development* **131**, 153-163.

Bilic, J., Huang, Y. L., Davidson, G., Zimmermann, T., Cruciat, C. M., Bienz, M. and Niehrs, C. (2007). Wnt induces LRP6 signalosomes and promotes dishevelled-dependent LRP6 phosphorylation. *Science* **316**, 1619-1622.

Brott, B. K. and Sokol, S. Y. (2005). Frodo proteins: modulators of Wnt signaling in vertebrate development. *Differentiation* **73**, 323-329.

Bryja, V., Andersson, E. R., Schambony, A., Esner, M., Bryjová, L., Biris, K. K., Hall, A. C., Kraft, B., Cajanek, L., Yamaguchi, T. P. et al. (2009). The extracellular domain of Lrp5/6 inhibits noncanonical Wnt signaling in vivo. *Mol. Biol. Cell* **20**, 924-936.

Caneparo, L., Huang, Y. L., Staudt, N., Tada, M., Ahrendt, R., Kazanskaya, O., Niehrs, C. and Houart, C. (2007). Dickkopf-1 regulates gastrulation movements by coordinated modulation of Wnt/beta catenin and Wnt/PCP activities, through interaction with the Dally-like homolog Knypek. *Genes Dev.* **21**, 465-480.

Cha, S. W., Tadjuidje, E., Tao, Q., Wylie, C. and Heasman, J. (2008). Wnt5a and Wnt11 interact in a maternal Dkk1-regulated fashion to activate both canonical and non-canonical signaling in Xenopus axis formation. *Development* **135**, 3719-3729.

Cong, F., Schweizer, L. and Varmus, H. (2004). Wnt signals across the plasma membrane to activate the beta-catenin pathway by forming oligomers containing its receptors, Frizzled and LRP. *Development* **131**, 5103-5115.

Cselenyi, C. S., Jernigan, K. K., Tahinci, E., Thorne, C. A., Lee, L. A. and Lee, E. (2008). LRP6 transduces a canonical Wnt signal independently of Axin degradation by inhibiting GSK3's phosphorylation of beta-catenin. *Proc. Natl. Acad. Sci. USA* **105**, 8032-8037.

Davidson, G., Wu, W., Shen, J., Bilic, J., Fenger, U., Stannek, P., Glinka, A. and Niehrs, C. (2005). Casein kinase 1 gamma couples Wnt receptor activation to cytoplasmic signal transduction. *Nature* **438**, 867-872.

Dibner, C., Elias, S. and Frank, D. (2001). XMeis3 protein activity is required for proper hindbrain patterning in Xenopus laevis embryos. *Development* **128**, 3415-3426.

Dibner, C., Elias, S., Ofir, R., Souopgui, J., Kolm, P. J., Sive, H., Pieler, T. and Frank, D. (2004). The Meis3 protein and retinoid signaling interact to pattern the Xenopus hindbrain. *Dev. Biol.* **271**, 75-86.

Djiane, A., Riou, J., Umbhauer, M., Boucaut, J. and Shi, D. (2000). Role of frizzled 7 in the regulation of convergent extension movements during gastrulation in Xenopus laevis. *Development* **127**, 3091-3100.

Elkouby, Y. M. and Frank, D. (2010). Wnt/β-catenin signaling in vertebrate posterior neural development. In *Colloquium Series on Developmental Biology* (ed. D. S. Kessler), eBook 4. San Rafael, CA: Morgan & Claypool Life Sciences.

Elkouby, Y. M., Elias, S., Casey, E. S., Blythe, S. A., Tsabar, N., Klein, P. S., Root, H., Liu, K. J. and Frank, D. (2010). Mesodermal Wnt signaling organizes the neural plate via Meis3. *Development* **137**, 1531-1541.

Elkouby, Y. M., Polevoy, H., Gutkovich, Y. E., Michaelov, A. and Frank, D. (2012). A hindbrain-repressive Wnt3a/Meis3/Tsh1 circuit promotes neuronal differentiation and coordinates tissue maturation. *Development* **139**, 1487-1497.

Fonar, Y., Gutkovich, Y. E., Root, H., Malyarova, A., Aamar, E., Golubovskaya, V. M., Elias, S., Elkouby, Y. M. and Frank, D. (2011). Focal adhesion kinase protein regulates Wnt3a gene expression to control cell fate specification in the developing neural plate. *Mol. Biol. Cell* **22**, 2409-2421.

Funato, Y., Michiue, T., Terabayashi, T., Yukita, A., Danno, H., Asashima, M. and Miki, H. (2008). Nucleoredoxin regulates the Wnt/planar cell polarity pathway in Xenopus. *Genes Cells* **13**, 965-975.

Golubkov, V. S. and Strongin, A. Y. (2012). Insights into ectodomain shedding and processing of protein-tyrosine pseudokinase 7 (PTK7). *J. Biol. Chem.* **287**, 42009-42018.

Gutkovich, Y. E., Ofir, R., Elkouby, Y. M., Dibner, C., Gefen, A., Elias, S. and Frank, D. (2010). Xenopus Meis3 protein lies at a nexus downstream to Zic1 and Pax3 proteins, regulating multiple cell-fates during early nervous system development. *Dev. Biol.* **338**, 50-62.

Hayes, M., Naito, M., Daulat, A., Angers, S. and Ciruna, B. (2013). Ptk7 promotes non-canonical Wnt/PCP-mediated morphogenesis and inhibits Wnt/β-catenin-dependent cell fate decisions during vertebrate development. *Development* **140**, 1807-1818.

Heasman, J., Kofron, M. and Wylie, C. (2000). β-catenin signaling activity dissected in the early Xenopus embryo: a novel antisense approach. *Dev. Biol.* **222**, 124-134.

Janssens, S., Denayer, T., Deroo, T., Van Roy, F. and Vleminckx, K. (2010). Direct control of Hoxd1 and Irx3 expression by Wnt/beta-catenin signaling during anteroposterior patterning of the neural axis in Xenopus. *Int. J. Dev. Biol.* **54**, 1435-1442.

Kofron, M., Birsoy, B., Houston, D., Tao, Q., Wylie, C. and Heasman, J. (2007). Wnt11/beta-catenin signaling in both oocytes and early embryos acts through LRP6-mediated regulation of axin. *Development* **134**, 503-513.

Kühl, M., Geis, K., Sheldahl, L. C., Pukrop, T., Moon, R. T. and Wedlich, D. (2001). Antagonistic regulation of convergent extension movements in Xenopus by Wnt/beta-catenin and Wnt/Ca2+ signaling. *Mech. Dev.* **106**, 61-76.

Lee, J., Andreeva, A., Sipe, C. W., Liu, L., Cheng, A. and Lu, X. (2012). PTK7 regulates myosin II activity to orient planar polarity in the mammalian auditory epithelium. *Curr. Biol.* **22**, 956-966.

Li, Y., Lu, W., King, T. D., Liu, C. C., Bijur, G. N. and Bu, G. (2010). Dkk1 stabilizes Wnt co-receptor LRP6: implication for Wnt ligand-induced LRP6 down-regulation. *PLoS ONE* **5**, e11014.

Lu, X., Borchers, A. G., Jolicoeur, C., Rayburn, H., Baker, J. C. and Tessier-Lavigne, M. (2004). PTK7/CCK-4 is a novel regulator of planar cell polarity in vertebrates. *Nature* **430**, 93-98.

MacDonald, B. T., Yokota, C., Tamai, K., Zeng, X. and He, X. (2008). Wnt signal amplification via activity, cooperativity, and regulation of multiple intracellular PPPSP motifs in the Wnt co-receptor LRP6. *J. Biol. Chem.* **283**, 16115-16123.

MacDonald, B. T., Tamai, K. and He, X. (2009). Wnt/beta-catenin signaling: components, mechanisms, and diseases. *Dev. Cell* **17**, 9-26.

Miller, M. A. and Steele, R. E. (2000). Lemon encodes an unusual receptor protein-tyrosine kinase expressed during gametogenesis in Hydra. *Dev. Biol.* **224**, 286-298.

Na, H. W., Shin, W. S., Ludwig, A. and Lee, S. T. (2012). The cytosolic domain of protein-tyrosine kinase 7 (PTK7), generated from sequential cleavage by a disintegrin and metalloprotease 17 (ADAM17) and γ-secretase, enhances cell proliferation and migration in colon cancer cells. *J. Biol. Chem.* **287**, 25001-25009.

Niehrs, C. (2004). Regionally specific induction by the Spemann-Mangold organizer. *Nat. Rev. Genet.* **5**, 425-434.
Niehrs, C. and Shen, J. (2010). Regulation of Lrp6 phosphorylation. *Cell. Mol. Life Sci.* **67**, 2551-2562.
Ohkawara, B. and Niehrs, C. (2011). An ATF2-based luciferase reporter to monitor non-canonical Wnt signaling in Xenopus embryos. *Dev. Dyn.* **240**, 188-194.
Paudyal, A., Damrau, C., Patterson, V. L., Ermakov, A., Formstone, C., Lalanne, Z., Wells, S., Lu, X., Norris, D. P., Dean, C. H. et al. (2010). The novel mouse mutant, chuzhoi, has disruption of Ptk7 protein and exhibits defects in neural tube, heart and lung development and abnormal planar cell polarity in the ear. *BMC Dev. Biol.* **10**, 87.
Penzo-Mendèz, A., Umbhauer, M., Djiane, A., Boucaut, J. C. and Riou, J. F. (2003). Activation of Gbetagamma signaling downstream of Wnt-11/Xfz7 regulates Cdc42 activity during Xenopus gastrulation. *Dev. Biol.* **257**, 302-314.
Peradziryi, H., Kaplan, N. A., Podleschny, M., Liu, X., Wehner, P., Borchers, A. and Tolwinski, N. S. (2011). PTK7/Otk interacts with Wnts and inhibits canonical Wnt signalling. *EMBO J.* **30**, 3729-3740.
Puppo, F., Thomé, V., Lhoumeau, A. C., Cibois, M., Gangar, A., Lembo, F., Belotti, E., Marchetto, S., Lécine, P., Prébet, T. et al. (2011). Protein tyrosine kinase 7 has a conserved role in Wnt/β-catenin canonical signalling. *EMBO Rep.* **12**, 43-49.
Re'em-Kalma, Y., Lamb, T. and Frank, D. (1995). Competition between noggin and bone morphogenetic protein 4 activities may regulate dorsalization during Xenopus development. *Proc. Natl. Acad. Sci. USA* **92**, 12141-12145.
Roszko, I., Sawada, A. and Solnica-Krezel, L. (2009). Regulation of convergence and extension movements during vertebrate gastrulation by the Wnt/PCP pathway. *Semin. Cell Dev. Biol.* **20**, 986-997.
Salzberg, A., Elias, S., Nachaliel, N., Bonstein, L., Henig, C. and Frank, D. (1999). A Meis family protein caudalizes neural cell fates in Xenopus. *Mech. Dev.* **80**, 3-13.
Saneyoshi, T., Kume, S., Amasaki, Y. and Mikoshiba, K. (2002). The Wnt/calcium pathway activates NF-AT and promotes ventral cell fate in Xenopus embryos. *Nature* **417**, 295-299.
Shnitsar, I. and Borchers, A. (2008). PTK7 recruits dsh to regulate neural crest migration. *Development* **135**, 4015-4024.
Snir, M., Ofir, R., Elias, S. and Frank, D. (2006). Xenopus laevis POU91 protein, an Oct3/4 homologue, regulates competence transitions from mesoderm to neural cell fates. *EMBO J.* **25**, 3664-3674.
Tahinci, E., Thorne, C. A., Franklin, J. L., Salic, A., Christian, K. M., Lee, L. A., Coffey, R. J. and Lee, E. (2007). Lrp6 is required for convergent extension during Xenopus gastrulation. *Development* **134**, 4095-4106.
Wallingford, J. B., Rowning, B. A., Vogeli, K. M., Rothbächer, U., Fraser, S. E. and Harland, R. M. (2000). Dishevelled controls cell polarity during Xenopus gastrulation. *Nature* **405**, 81-85.
Wallingford, J. B., Fraser, S. E. and Harland, R. M. (2002). Convergent extension: the molecular control of polarized cell movement during embryonic development. *Dev. Cell* **2**, 695-706.
Wang, Y. (2009). Wnt/Planar cell polarity signaling: a new paradigm for cancer therapy. *Mol. Cancer Ther.* **8**, 2103-2109.
Wehner, P., Shnitsar, I., Urlaub, H. and Borchers, A. (2011). RACK1 is a novel interaction partner of PTK7 that is required for neural tube closure. *Development* **138**, 1321-1327.
Weidenfeld-Baranboim, K., Koren, L. and Aronheim, A. (2011). Phosphorylation of JDP2 on threonine-148 by the c-Jun N-terminal kinase targets it for proteosomal degradation. *Biochem. J.* **436**, 661-669.
Yan, D., Wallingford, J. B., Sun, T. Q., Nelson, A. M., Sakanaka, C., Reinhard, C., Harland, R. M., Fantl, W. J. and Williams, L. T. (2001). Cell autonomous regulation of multiple Dishevelled-dependent pathways by mammalian Nkd. *Proc. Natl. Acad. Sci. USA* **98**, 3802-3807.
Yen, W. W., Williams, M., Periasamy, A., Conaway, M., Burdsal, C., Keller, R., Lu, X. and Sutherland, A. (2009). PTK7 is essential for polarized cell motility and convergent extension during mouse gastrulation. *Development* **136**, 2039-2048.
Zeng, X., Huang, H., Tamai, K., Zhang, X., Harada, Y., Yokota, C., Almeida, K., Wang, J., Doble, B., Woodgett, J. et al. (2008). Initiation of Wnt signaling: control of Wnt coreceptor Lrp6 phosphorylation/activation via frizzled, dishevelled and axin functions. *Development* **135**, 367-375.
Zetser, A., Frank, D. and Bengal, E. (2001). MAP kinase converts MyoD into an instructive muscle differentiation factor in Xenopus. *Dev. Biol.* **240**, 168-181.